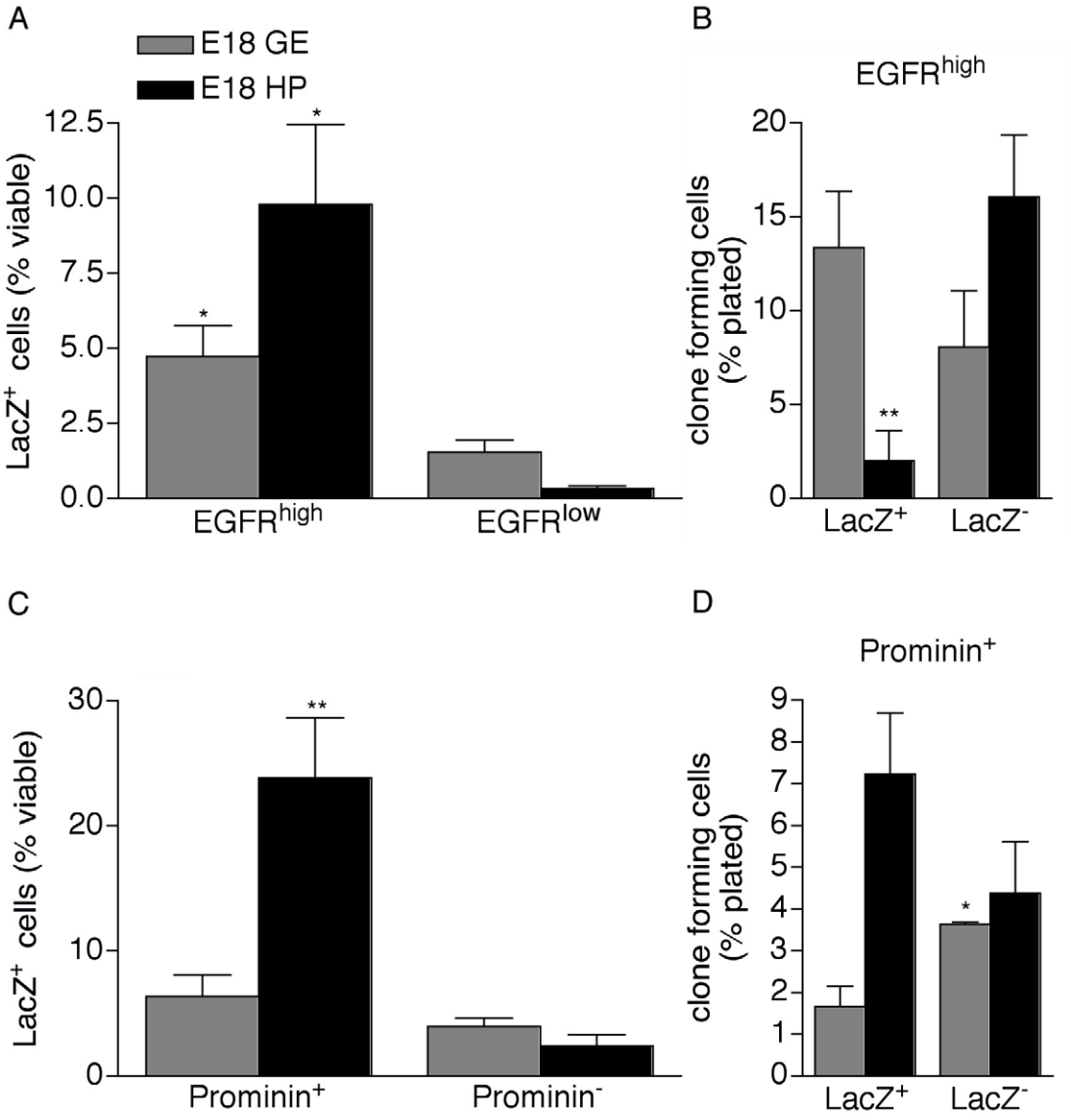

Supplementary Figure 1: In the E18 HP *Gdf15* expressing cells include a subset of neural stem cells. (A and C) Percentage of cells displaying β-galactosidase activity ($LacZ^+$) in the dissociated cells of the E18 *Gdf15*$^{+/-}$ GE and HP sorted according to levels of expression of EGFR (A) and Prominin (C). (B and D) Quantitative analysis of the clone-forming activity in cells sorted on the EGFR (B) or Prominin (D) expression and LacZ activity. * indicate significantly different from the corresponding $EGFR^{low}$ (A), $Prominin^-$ (C), $LacZ^-$ (B, D) population. *: $P \leq 0.05$; ** $P \leq 0.01$, $n \geq 5$.

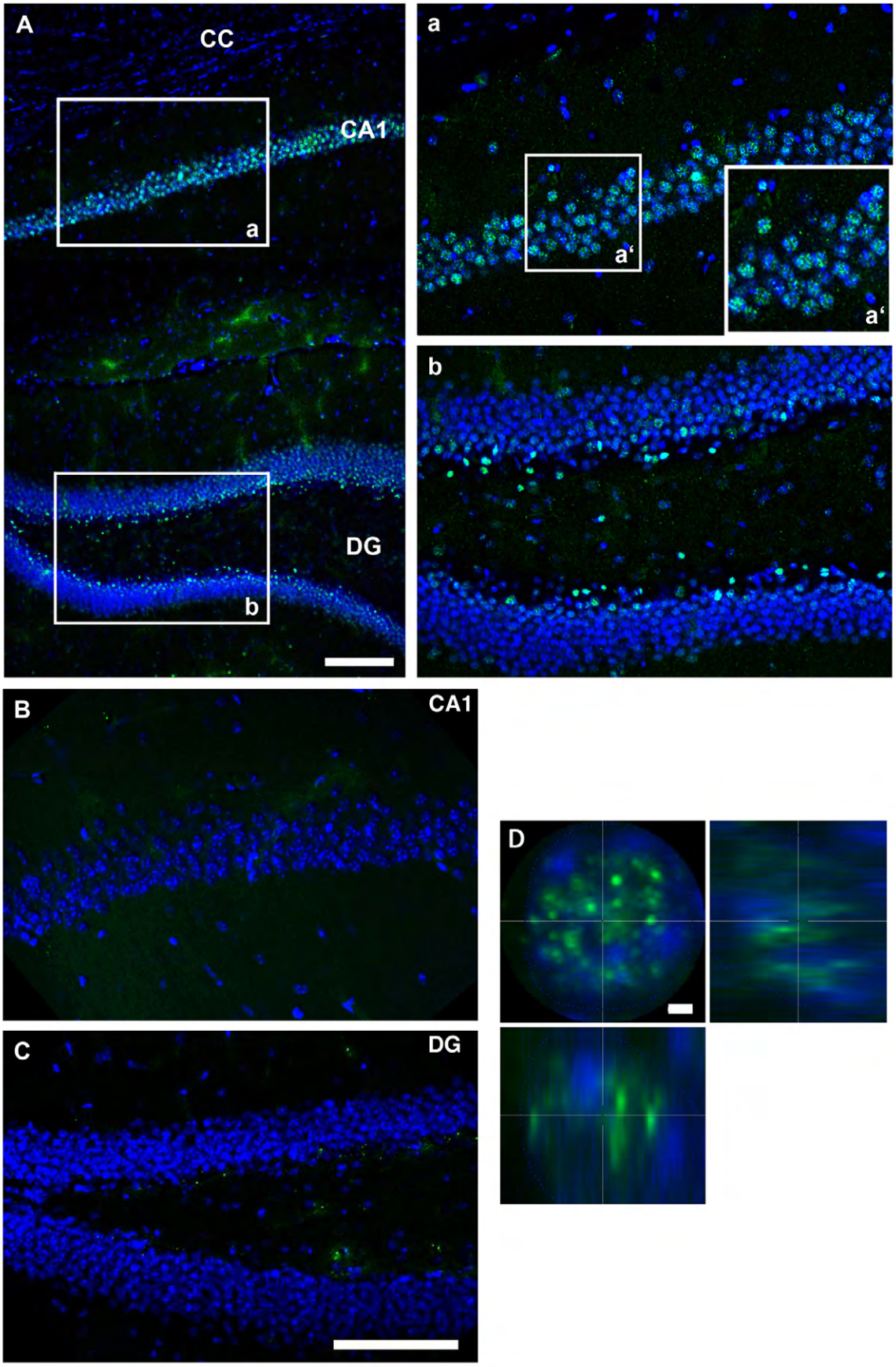

Supplementary Figure 2: Expression of GDF-15 protein in the adult HP. Representative photomicrographs illustrating coronal sections of the WT (A) and *Gdf15*$^{-/-}$ (B, C) CA1 (A, B) and DG (A, C) after immunostaining with α-GDF-15 (green fluorescence). (a), (b) and (a') show higher magnifications of the boxed areas in (Aa), (Ab) and (a), respectively. DAPI counterstaining of the nuclei is shown in blue. Orthogonal projections of a GDF-15^{+} nucleus were obtained at a magnification of ~200x to assess localization (D). Scale bars are 100 µm in A-C and 1 µm in D.

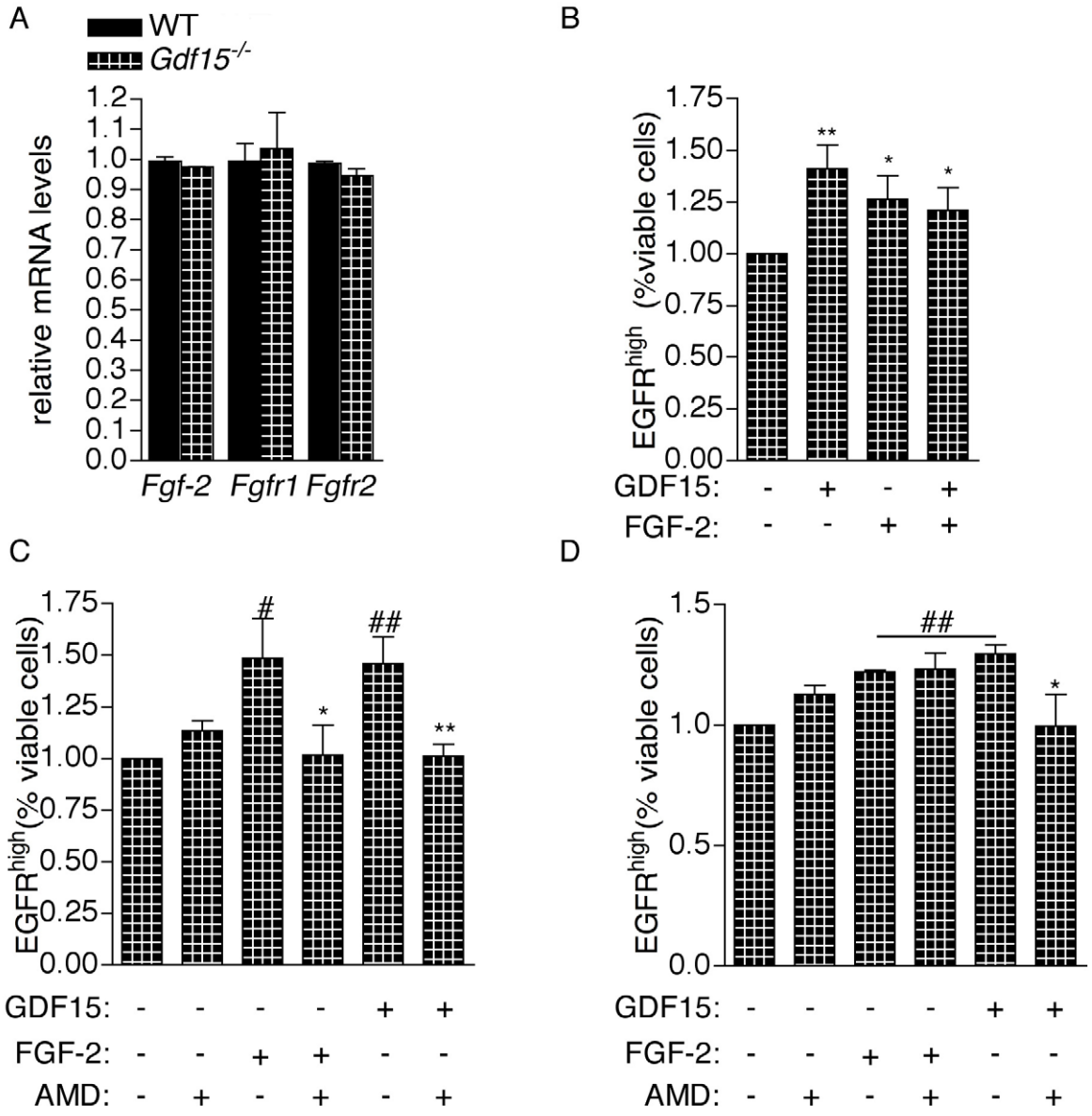

Supplementary Figure 3: GDF-15 modulates EGFR expression independently of FGF signalling. (A) Comparison of *Fgf-2*, *Fgfr1* and *Fgfr2* mRNA levels relative to *Gapdh* and β-Actin mRNAs in WT and *Gdf15*$^{-/-}$ HP. (B-D) Quantitative analysis of the number of EGFR^{high} cells isolated from the E18 *Gdf15*$^{-/-}$ HP after incubation for 6 (B-C) and 24 (D) hours in the presence and/or absence of exogenous growth factors and CXCR-4 blocker AMD3100 as indicated. * denotes significantly different from control cells not exposed to growth factors (B) and counterparts not treated with AMD3100 (C, D). # denotes significantly different from cells exposed to neither growth factors nor AMD3100.*,#: $P \leq 0.05$. **,##: $P \leq 0.01$; $n \geq 3$.

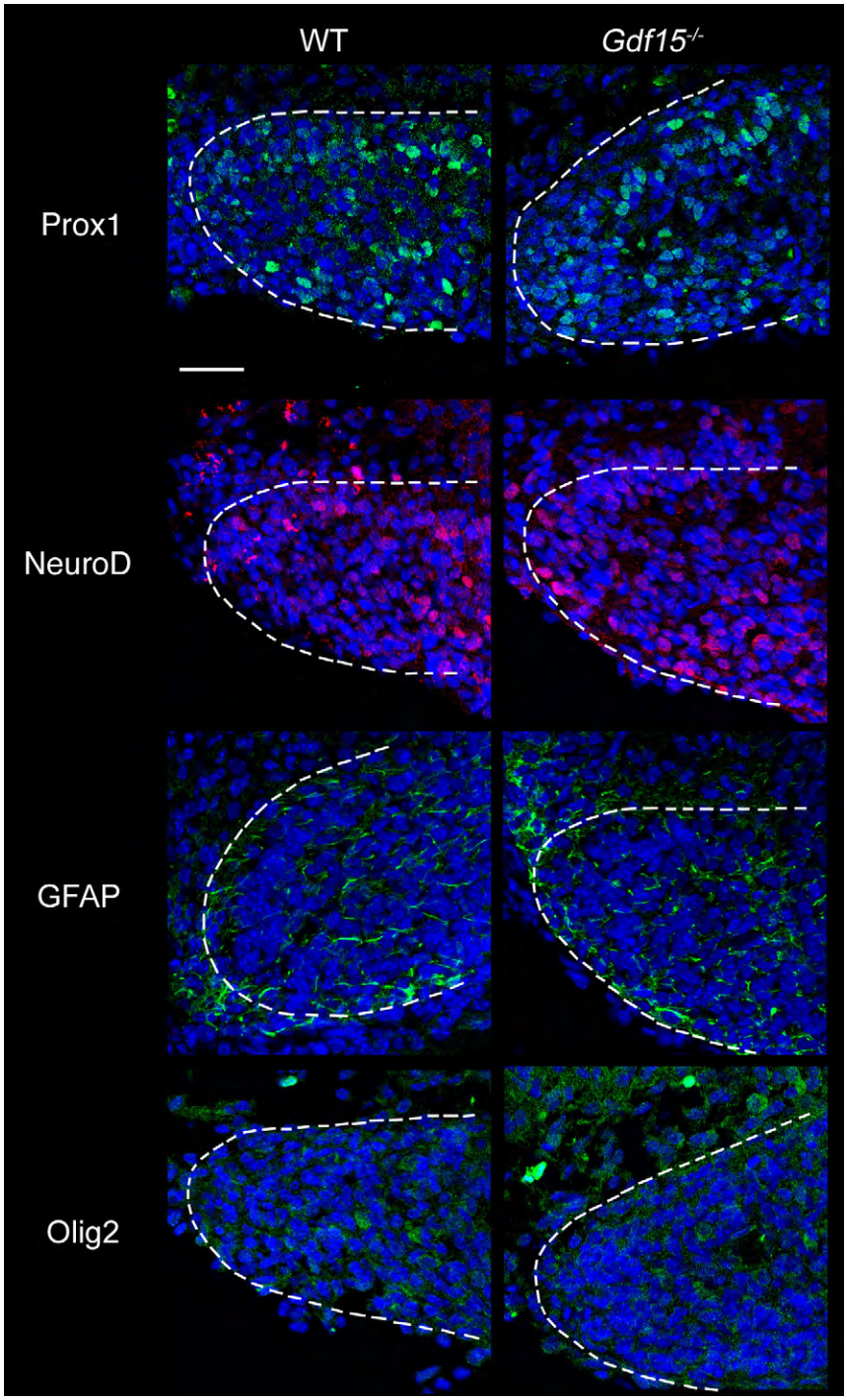

Supplementary Figure 4: Qualitative analysis of the expression of the indicated antigens in E18 WT and *Gdf15*$^{-/-}$ HP by immunostaining. DAPI counterstaining of the nuclei is shown in blue. Scale bar is 37.5mm.

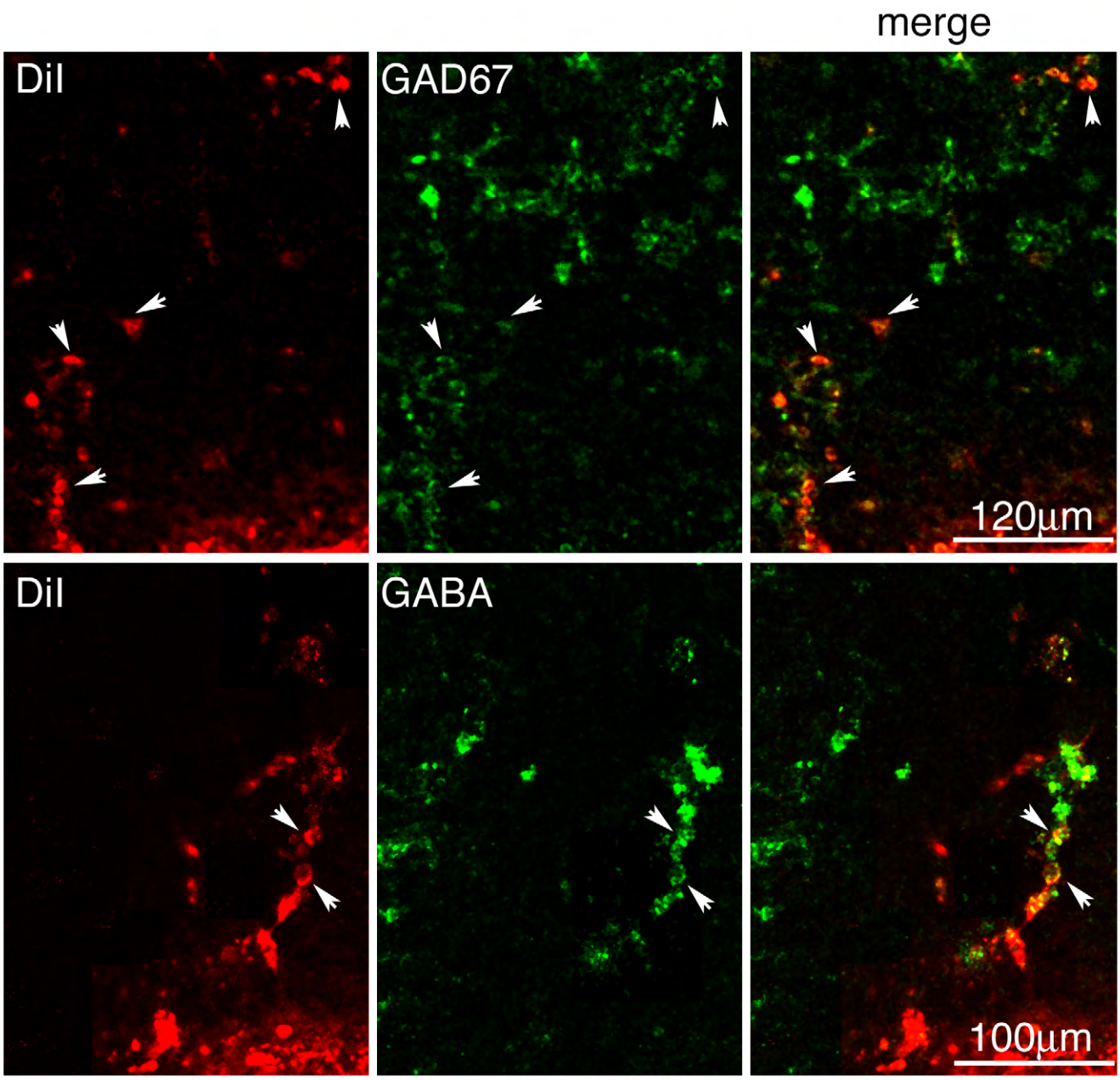

Supplementary Figure 5: Representative micrographs showing immunoreactivity to GAD67 and GABA antibodies of DiI-labelled cells in the CA1 in organotypic slices of the E18 HP that had been cultured *in vitro* for 3 days.

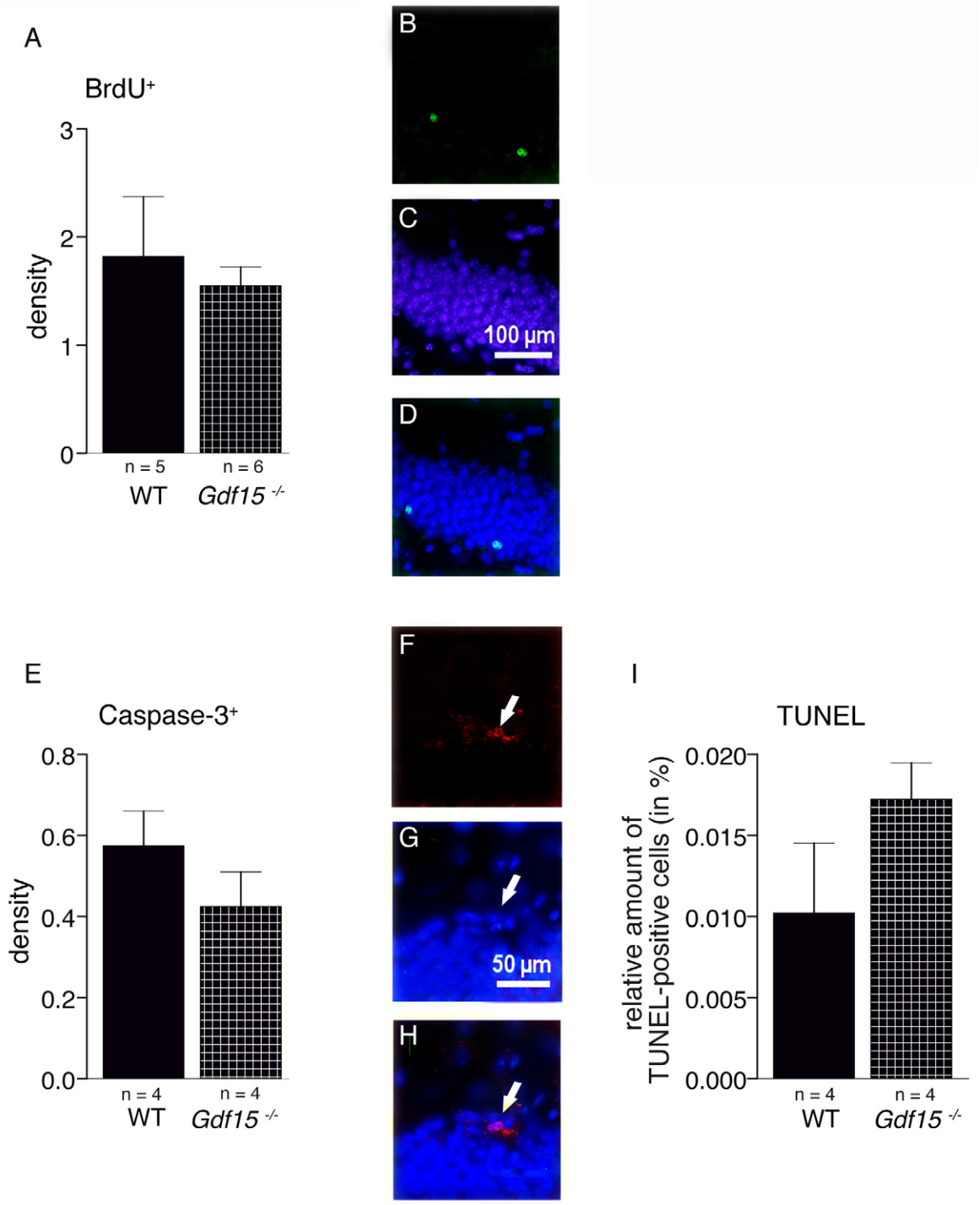

Supplementary Figure 6: Proliferation and cell death in the HP of 6 month-old mice are not affected by the genotype. (A) Quantitative analysis of the number of BrdU immunopositive cells in WT and *Gdf15*$^{-/-}$ in the DG of 6 month-old animals. Data are expressed as means of the number of cells per slice. (B-D) representative images of BrdU-labelled cells (B) DAPI counterstained of nuclei (C) and merge (D) within the DG. (E) Densities of activated caspase 3 positive cells were not altered in 6 month-old *Gdf15*$^{-/-}$ animals, indicating no effect of the genotype on apoptosis. (F-H) representative images of activated caspase-3-labelled cells (F) DAPI cell nuclei (G) and merge (H) within the DG. (I) TUNEL-experiments also demonstrate no significant change in the rate of apoptosis.

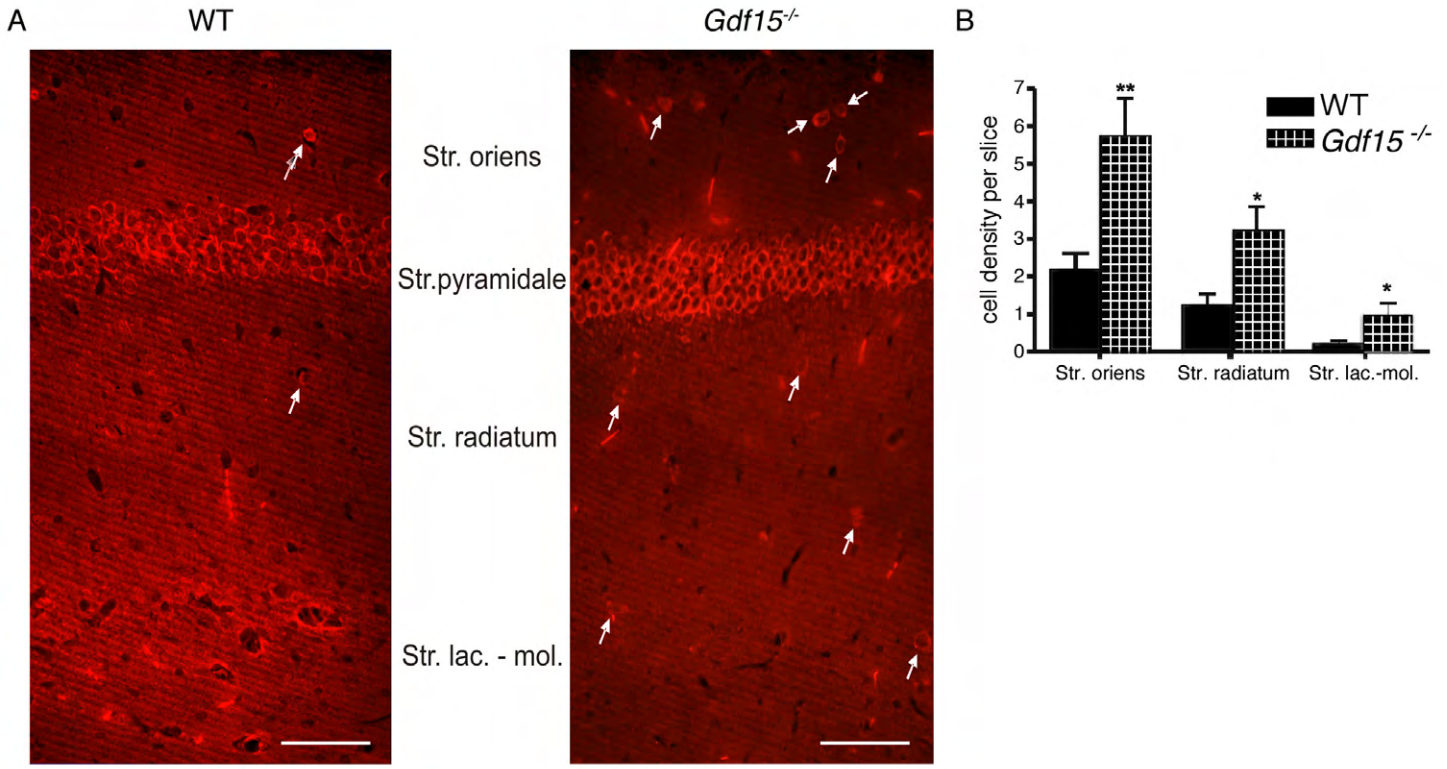

Supplementary Figure 7: Adult *Gdf15*$^{-/-}$ mice show neuronal alteration within the hippocampal area CA1. (A) Representative photomicrographs showing immunostaining for CamKIIα in the CA1 of WT and *Gdf15*$^{-/-}$ 6 month-old animals. Arrows point to some CamKIIα^{+} cells. Scale bar is 100 µm. (B) Quantification of the cell densities of CamKIIα^{+} cells in different layers of the CA1 region. * indicate significantly different from WT counterpart values. *: P≤0.05; **P:≤0.01; n≥3.